DALTON
FULL PAPER

A phase transition in the novel three-dimensional compound $[Eu_2(mal)_3(H_2O)_6]$ (H_2mal = malonic acid)

María Hernández-Molina,[a] Pablo Lorenzo-Luis,[b] Catalina Ruiz-Pérez,*[a] Trinidad López,[c] Inocencio R. Martín,[d] Kirsty M. Anderson,[e] A. Guy Orpen,[e] Eduardo H. Bocanegra,[f] Francesc Lloret[g] and Miguel Julve[g]

[a] *Laboratorio de Rayos X y Materiales Moleculares. Dpto de Física Fundamental II, Avda. Astrofisico Francisco Sánchez s/n, Facultad de Física, Universidad de La Laguna, 38204-La Laguna, Tenerife, Spain. E-mail: caruiz@ull.es*
[b] *Dpto de Química Inorgánica, Universidad de La Laguna, 38204-La Laguna, Tenerife, Spain*
[c] *Dpto de Física Básica, Facultad de Física, Universidad de La Laguna, 38204-La Laguna, Tenerife, Spain*
[d] *Dpto de Física Fundamental y Experimental, Universidad de La Laguna, 38204-La Laguna, Tenerife, Spain*
[e] *School of Chemistry, University of Bristol, Bristol, UK BS8 1TS*
[f] *Dpto de Física Aplicada, Facultad de Ciencias, Universidad de País Vasco, Spain*
[g] *Dpto de Química Inorgánica/Instituto de Ciencia Molecular, Facultad de Química de la Universitat de Valècia, Dr. Moliner 50, 46100-Burjassot, (València), Spain*

Received 15th March 2002, Accepted 29th May 2002
First published as an Advance Article on the web 23rd August 2002

Slow diffusion of aqueous solutions of europium(III) chloride into gel of sodium metasilicate containing malonic acid (H_2mal) yields single crystals of the three-dimensional compound of formula $[Eu_2(mal)_3(H_2O)_6]$ whose structure was determined by X-ray diffraction methods at 293 and 173 K. It crystallizes in the monoclinic system but the spatial group changes from *I2/a* in the high temperature range ($293 \geq T \geq 236$ K) to *Ia* in the low temperature range ($T < 236$ K). In both cases, nine oxygen atoms forming a distorted monocapped square antiprism surround the Eu^{3+} ions. The structure at 293 K consists of a three-dimensional arrangement of triaquaeuropium(III) units bridged by malonate groups which result from cross-linking of the single chains running parallel to the *c* axis and the double zig-zag chains which grow in the *ab* plane. At low temperature the structure of the compound can be visualised as chains of europium(III) ions linked through two of the three crystallographically independent malonate ligands, whose chains run parallel to the *b* axis and a second family of chains (along the *c* axis) through the third independent malonate ligand forming a three-dimensional network. In both the crystal structure is stabilised through extensive hydrogen bonding involving carboxylate and water molecules. Studies of the magnetic behaviour, spectroscopic, thermogravimetric and calorimetric characteristics of $[Eu_2(mal)_3(H_2O)_6]$ are reported. Laser-excited site selective spectroscopy shows a unique crystal-field site for Eu^{III} ions in the crystal at room temperature and down to 236 K. However, below this temperature, two different sites are clearly identified, in agreement with a change in the crystal structure.

Introduction

Metal coordination polymers with one-, two- and three-dimensional frameworks have been the subject of intensive research for several decades. Major advances have been made in their synthesis, theoretical description and in their applications as new materials.[1] The chemistry of metal coordination polymers is among one of the most promising interfaces between synthetic chemistry and materials science. In this context, the field is important as it provides a foundation for the understanding of molecular organisation in the solid state. The structural design or modification of frameworks has become a very active field of crystal engineering. An example of the advance in this field is the generation of polymeric structures in metal complexes using di-carboxylate-ligands, which develop theoretical models of the exchange interaction in extended lattices.[2]

Recent studies show that the flexibility of the molecular backbones, their conformational preferences, the metal ions employed and their counter ions, all have a profound influence on the polymeric structures obtained.[2] In our work we have used the malonate dianion (*i.e* the dianion of malonic acid, hereafter denoted mal) as a bridging ligand in metal complexes because of its ability to form extended networks. The structures formed — which depend on factors such as type of metal, the nature of the organic functionality of the ligand and reaction conditions — are mostly polymeric; either chains or two- and three-dimensional networks.[3]

The expansion of research activity in the chemistry of malonic acid derivatives as ligands for lanthanide and transition metals, reflects the growing interest in their practical applications as fluorescence probes[4] and molecular magnetic materials[3] as well as precursors for oxides.[5] Therefore, studies of the new complexes of lanthanides with malonic acid are important both inherently and in their applications.

There are six isostructural series in the malonate-containing lanthanide complexes of general formula $[Ln_2(mal)_3(H_2O)_n]\cdot mH_2O$ and $[Ln(mal)_2]\cdot pH_2O$ with Ln = lanthanide element, $n = 2$ ($m = 3$ and 4) and 5 ($m = 3$) and $p = 3$, 4 and 5, where the total number of water molecules and the oxidation state of the rare earth element are structure determining factors.[3a,4,6–8] To the best of our knowledge, the only example reported to date of

 DOI: 10.1039/b202649j

a malonate complex with europium(III), $[Eu_2(mal)_3(H_2O)_5]\cdot 3H_2O$, belongs to this family and has the greater number of coordinated water molecules.[6] Its structural determination by X-ray crystallography on single crystals confirmed the presence of an orthorhombic structure with space group *Pnma* at room temperature. In the framework of our studies concerning the coordinating ability of malonate with metal ions,[3b–i] we obtained single crystals of a three-dimensional malonate complex with Eu(III) of formula $[Eu_2(mal)_3(H_2O)_6]$. This compound crystallizes in the monoclinic system and exhibits a phase transition as a function of temperature. We report here its crystal structure (high and low temperature phases), thermogravimetric and calorimetric studies as well as the investigation of fluorescence and magnetic properties.

Results and discussion

Description of the structure of $[Eu_2(mal)_3(H_2O)_6]$ 1

High temperature phase. The structure of complex **1** at 293 K consists of a three-dimensional arrangement of triaquaeuropium(III) units bridged by malonate groups (see Fig. 1) which results from the cross-linking of the single chains running parallel to the *c* axis (Fig. 2a) and the double zig-zag chains

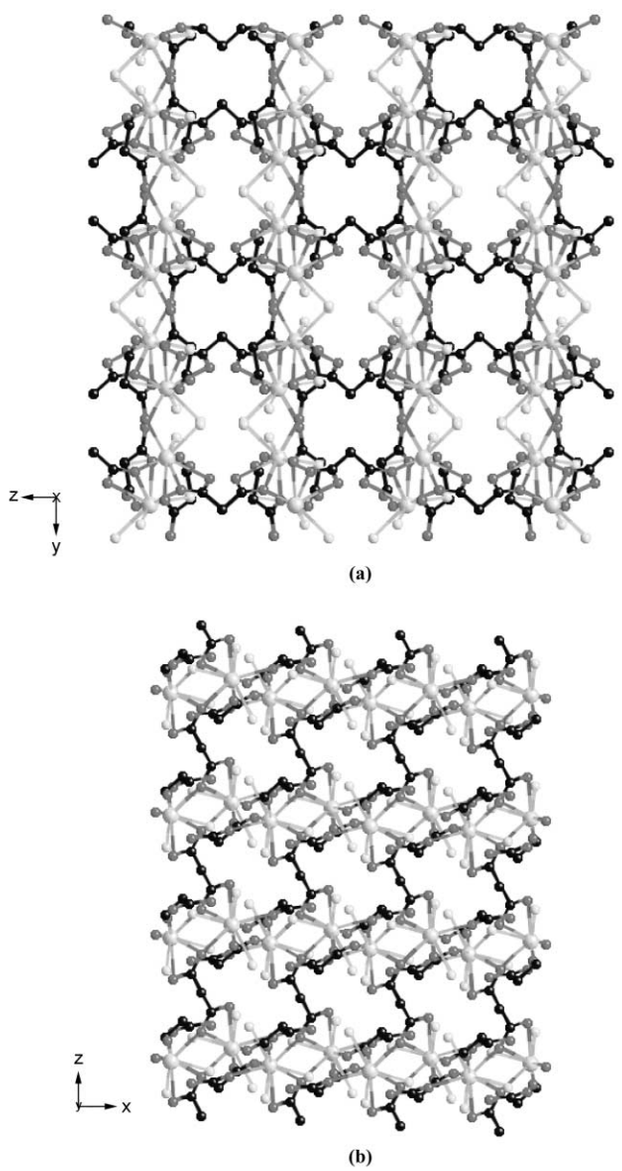

Fig. 1 View of the three-dimensional structure of $[Eu_2(mal)_3(H_2O)_6]$ at 293 K: (a) along the *a* axis and (b) along the *b* axis. Hydrogen atoms have been omitted for the sake of clarity.

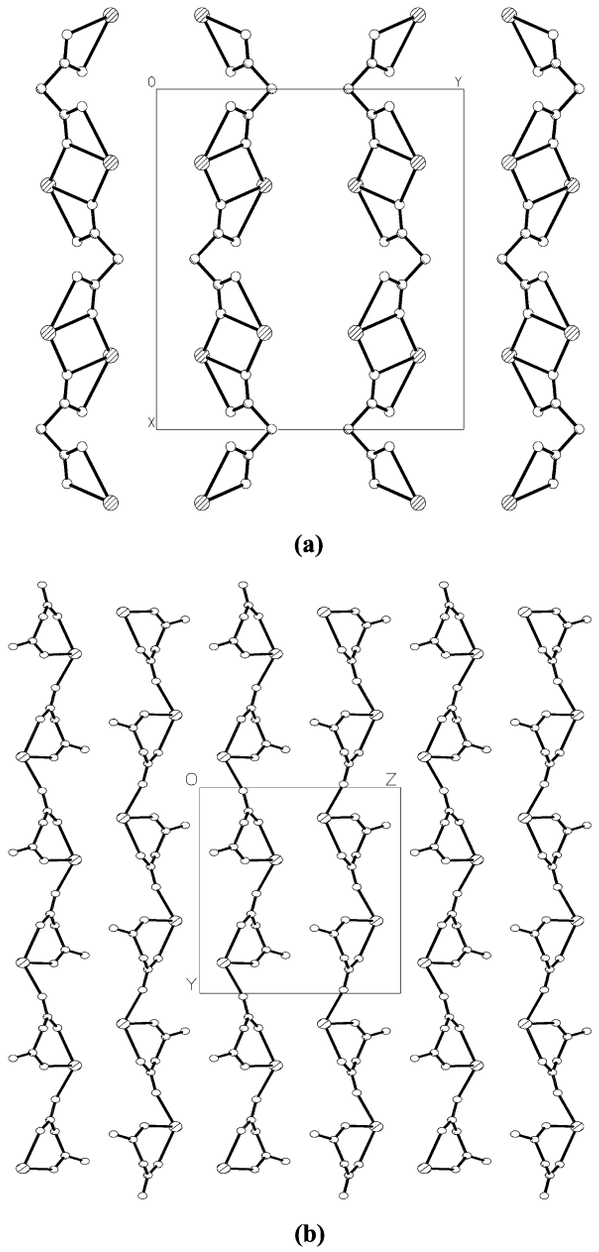

Fig. 2 $[Eu_2(mal)_3(H_2O)_6]$ at 293 K. (a) Projection of the double chains down the *b* axis. Water molecules, malonate ligand L1 and hydrogen atoms have been omitted for clarity. (b) Projection of the single chains down the *c* axis. Water molecules, malonate ligand L2 and hydrogen atoms have been omitted for clarity.

which grow in the *ab* plane (Fig. 2b). Extensive hydrogen bonds involving carboxylate groups and the water molecules contributes to the stabilisation of the crystal structure (see end of Table 1).

The Eu atom in $[Eu_2(mal)_3(H_2O)_6]$ at 293 K is surrounded by nine oxygen atoms forming a distorted monocapped square antiprism (see Fig. 3a). Similar geometries are observed in other lanthanide–malonate complexes.[3a,4,6–8] The nine oxygen atoms around Eu1 are provided by three malonate ligands and three coordinated water molecules as shown in Table 1 and Fig. 4a. Three points deserve to be outlined from the analysis of the data listed in Table 1: (i) firstly, the average value of the Eu1–O bond distances is 2.519(5) Å, shorter than found for $[Eu_2(mal)_3(H_2O)_5]\cdot 3H_2O$[6] [2.54(2) Å]. (ii) Secondly, the existence of a long bond, 2.597(5) Å, between Eu1 and the O6 atom of the carboxylate group C4O5O6, accompanies the formation of the oxygen bridge Eu(1)–O(6)–Eu(1)b (b = 3/2 − *x*, 3/2 − *y*, 1/2 − *z*) (Fig. 4a), which is significantly different to that found for $[Eu_2(mal)_3(H_2O)_5]\cdot 3H_2O$ [2.84(2) Å].[6] Similar asymmetric

Table 1 Dimensions (Å) of the coordination polyhedron for $[Eu_2(mal)_3(H_2O)_6]$

293 K		173 K			
Eu(1)–O(1)	2.353(6)	Eu(1)–O(1)	2.329(4)	Eu(2)–O(4)e	2.287(4)
Eu(1)–O(2)	2.415(5)	Eu(1)–O(3)	2.406(4)	Eu(2)–O(5)	2.408(4)
Eu(1)–O(3)a	2.310(5)	Eu(1)–O(8)c	2.317(4)	Eu(2)–O(7)	2.430(3)
Eu(1)–O(5)	2.532(5)	Eu(1)–O(9)	2.585(7)	Eu(2)–O(9)	2.457(8)
Eu(1)–O(6)	2.597(5)	Eu(1)–O(10)	2.527(7)	Eu(2)–O(11)d	2.605(7)
Eu(1)–O(6)b	2.430(5)	Eu(1)–O(11)d	2.418(8)	Eu(2)–O(12)d	2.585(7)
Eu(1)–O(1W)	2.476(6)	Eu(1)–O(1W)	2.542(4)	Eu(2)–O(4W)	2.504(5)
Eu(1)–O(2W)	2.499(6)	Eu(1)–O(2W)	2.496(4)	Eu(2)–O(5W)	2.459(4)
Eu(1)–O(3W)	2.517(5)	Eu(1)–O(3W)	2.404(5)	Eu(2)–O(6W)	2.604(5)

Hydrogen bonds distances [Å] for $[Eu_2(mal)_3(H_2O)_6]$

293 K		173 K	
D ··· A	D ··· A	D–H ··· A	D ··· A
O(1W) ··· ·O(1)f	2.7816(8)	O(1W)–H(11) ··· O(6)i	2.7740
		O(1W)–H(12) ··· O(10)j	2.8257
O(1W) ··· O(2)b	2.7094(12)		
O(2W) ··· O(4)f	2.7550(8)	O(2W)–H(21) ··· O(7)e	2.7636
O(2W) ··· O(2W)g	2.7829(14)	O(2W)–H(22) ··· O(1)k	2.8032
O(3W) ··· O(3)a	2.8112(8)	O(3W)–H(31) ··· O(2)k	2.7731
O(3W) ··· O(4)h	2.7076(11)	O(3W)–H(32) ··· O(6W)l	2.7588
		O(4W)–H(41) ··· O(12)e	2.8503
		O(5W)–H(51) ··· O(3)i	2.6718
		O(5W)–H(52) ··· O(5)i	2.8190
		O(5W)–H(52) ··· O(6)i	3.2881
		O(6W)–H(61) ··· O(6)i	2.7435
		O(6W)–H(62) ··· O(3W)d	2.7588

Symmetry transformation used to generate equivalent atoms: a = 1 − *x*, 1/2 + *y*, 1/2 − *z*; b = 3/2 − *x*, 3/2 − *y*, 1/2 − *z*; c = 1/2 − *x*, −*y*, *z*; d = *x*, 1/2 − *y*, *z* − 1/2; e = *x* − 1/2, 1 − *y*, *z*; f = 1/2 + *x*, 2 − *y*, *z*; g = 1 − *x*, 2 − *y*, −*z*; h = 1/2 − *x*, 3/2 − *y*, 1/2 − *z*; i = 1/2 + *x*, 1 − *y*, *z*; j = *x* − 1/2, *y* − 1/2, *z* − 1/2; k = *x* − 1/2, −*y*, *z*; l = *x*, 1/2 − *y*, 1/2 + *z*.

oxygen bridges are found in other lanthanoid carboxylate structures.[3a,4,6–10] (iii) Thirdly, the europium to water oxygen bond lengths are in the range 2.476(6)–2.517(5) Å; these are on average slightly longer than that of europium to carboxylate oxygens [2.310(5)–2.532(5) Å]. This is consistent with the coordination ability of water being weaker than that of the carboxylates, in agreement with the thermogravimetric measurements discussed below.

Two malonate units are crystallographically independent and with different arrangements: L1 and L2, as shown in Scheme 1.

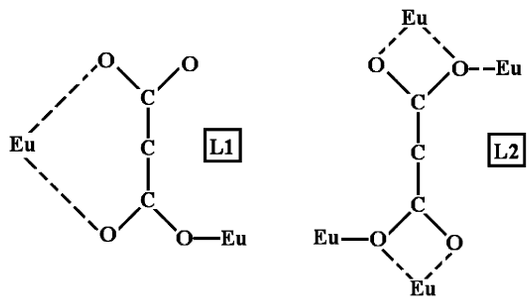

Scheme 1 Two bonding modes observed according to the coordination environment of the CO_2^- groups.

The L1 mode is characterised by the malonate ligand bridging two europium atoms acting as both a bidentate chelate ($^-O_2CCH_2CO_2^-$) and monodentate (^-O_2C–) ligand to europium. The chelate ring has a boat conformation while the monodentate function adopts an *anti–syn* conformation. In the L2 arrangement, the malonate ligand bridges four europium atoms through two bidentate four-membered chelate-rings as well as two monodentate interactions of *anti–anti* conformation. The average C–O bond distances and O–C–O bond angles, in both malonate ligands, are 1.253(8) Å and 122.3(5)°, respectively. These values are in agreement with other previously reported malonate–lanthanide complexes.[3a,4,6–10]

Two Eu ··· Eu separations are found, one Eu(1) ··· Eu(1)b (b = 3/2 − *x*, 3/2 − *y*, 1/2 − *z*) 4.275(1) Å bridged by the O(6) atom of carboxylate group C(4)O(5)O(6), as shown in Fig. 4a, and the other Eu(1) ··· Eu(1)m (m = 1/2 − *x*, 1/2 − *y*, 1/2 − *z*) 6.564(2) Å.

Low temperature phase. The structure of the compound can be visualised as chains of europium(III) ions linked through two of the three crystallographically independent malonate ligands, L1A and L1B (Fig. 5a), whose chains run parallel to the *b* axis. Both malonate ligands show the same conformation, of L1 type (see Scheme 1). A second family of chains (along the *c* axis) through the independent ligand L2A (Fig. 5b) are linked forming a three-dimensional network (Fig. 6). The crystal structure is stabilised through extensive hydrogen bonding involving carboxylate and water molecules (Table 1).

Two crystallographically independent europium(III) ions, Eu(1) and Eu(2), are found [Fig. 3b: Eu(1) (top) and Eu(2) (bottom)]. As in the structure at 293 K, nine oxygens atoms forming a distorted end-capped antiprism surround both. The coordination polyhedra are shown in Fig. 3b, and share corners formed by the O(9) and O(11)d (d = *x*, 1/2 − *y*, *z* − 1/2) atoms. The nine coordinated oxygen atoms are made up of six from three malonate ligands and three from water molecules (Table 1). From Table 1, the Eu–O bond distances are in the range 2.317(4)–2.585(7) Å for Eu(1) and 2.287(4)–2.605(7) Å for Eu(2). Their average values are 2.447(5) Å for Eu(1) and 2.482(5) Å for Eu(2). The distance Eu(1) ··· Eu(2) through the μ-oxygen bridge is 4.2799(4) and the next shortest Eu ··· Eu distance is 7.0966(5) Å (Fig. 4b).

In contrast to the room temperature structure described above, there are three crystallographically independent malonate ligands in the low temperature structure: two (L1A and L1B) have the L1 mode of bonding (see Scheme 1) and one

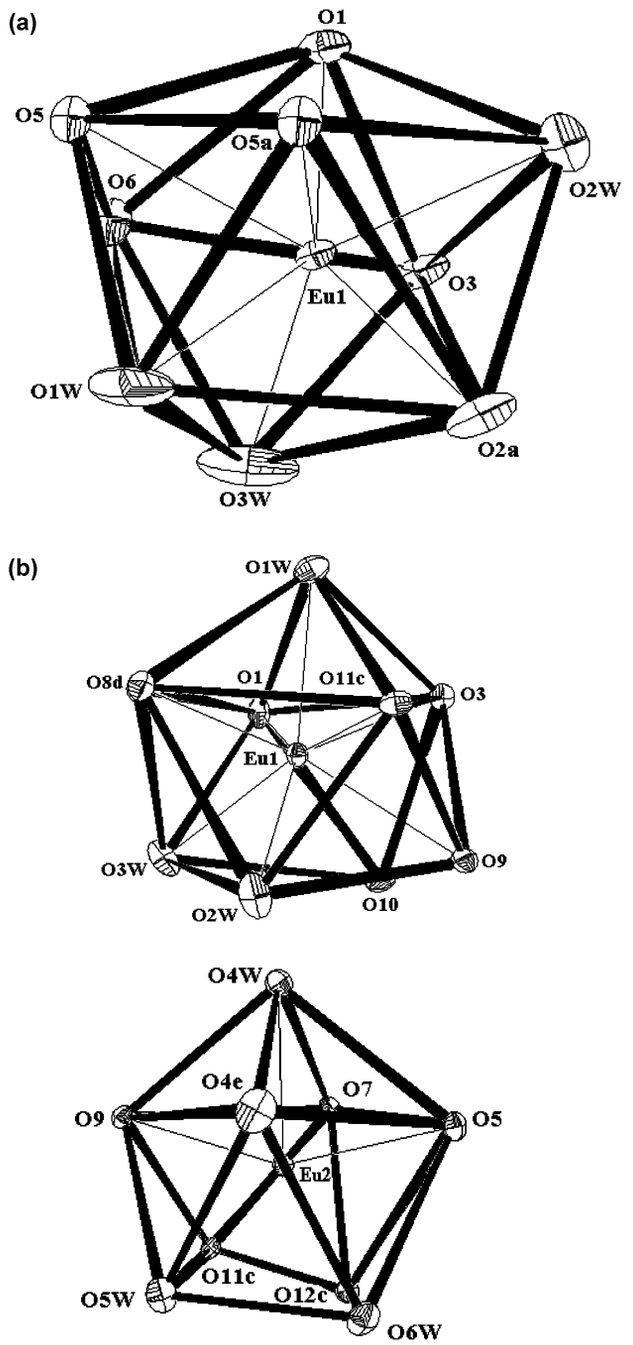

Fig. 3 Perspective drawing of europium ion environments (a) at 293 and (b) at 173 K. Hydrogen atoms have been omitted for clarity. Thermal ellipsoids are drawn at the 50% probability level. Symmetry codes: a = 1 − *x*, 1/2 + *y*, 1/2 − *z*; b = 3/2 − *x*, 3/2 + *y*, 1/2 − *z*; c = *x*, 1/2 − *y*, *z* − 1/2; d = 1/2 + *x*, −*y*, *z*; e = *x* − 1/2, 1 − *y*, *z*.

(L2A) has the L2 mode (see Scheme 1). The L1-type malonates chelate Eu(1) and Eu(2) and exhibit boat conformations. The carboxylate groups C(3)O(3)O(4) (L1A) and C(5)O(7)O(8) (L1B), adopt a monodentate coordination mode at Eu(1)k (k = *x* − 1/2, −*y*, *z*) and at Eu(2)i (i = 1/2 + *x*, 1 − *y*, *z*), respectively, exhibiting *anti–syn* conformations. The average C–O bond distances and O–C–O bond angles are 1.257(6) Å and 123.3(5)° for L1A and L1B, and 1.259(13) Å and 121.0(9)° for L2. These values are in agreement with other malonate complexes (as noted above).

Magnetic properties. The ground state for Eu^{III} is $^7F_0$, which is split by spin–orbit coupling into seven levels, ^7F_J, where J can take all values between 0 and 6. The spin–orbit Hamiltonian is expressed in the form $H_{S-O} = \lambda LS = \lambda(J^2 - L^2 - S^2)/2$;

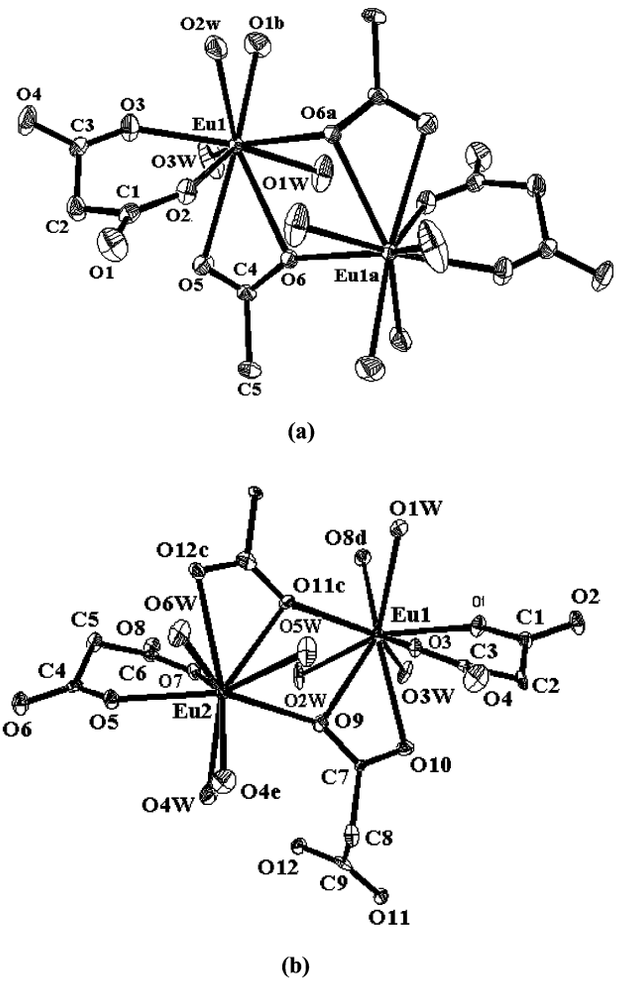

Fig. 4 Coordination geometry of the europium cation. (a) in $[Eu_2(mal)_3(H_2O)_6]$ at 293 K and (b) in $[Eu_2(mal)_3(H_2O)_6]$ at 173 K. Thermal ellipsoids are drawn at the 50% probability level. Symmetry codes: a = 1 − *x*, 1/2 + *y*, 1/2 − *z*; b = 3/2 − *x*, 3/2 − *y*, 1/2 − *z*; c = *x*, 1/2 − *y*, *z* − 1/2; d = 1/2 + *x*, −*y*, *z*; e = *x* − 1/2, 1 − *y*, *z*.

where the energies of the corresponding states are given by the equation $E(J) = \lambda\ (J + 1)/2$. Since λ is quite small, on the order of 300 cm^{-1}, the first excited state has a relative energy comparable to kT and there will be a significant thermal population. The magnetic susceptibility may be expressed in the form[11]

$$\chi = \frac{\sum_{J=0}^{6} (2J+1)\chi(J)\exp[-\lambda J(J+1)/2kT]}{\sum_{J=0}^{6} (2J+1)\exp[-\lambda J(J+1)/2kT]}$$

and $\chi(J)$ is given by the equation below

$$\chi(J) = \frac{N\beta^2 g_J^2 J(J+1)}{3kT} + \frac{2N\beta^2(g_J - 1)(g_J - 2)}{3\lambda}$$

In the present case the various g factors, g_J, are equal to 3/2, except for the ground state where $g_0 = 5$. Operating on the previous equations the definitive expression from the magnetic susceptibility is:

$$\chi = \frac{N\beta^2}{3kTx}\frac{A}{B} \qquad (1)$$

where $x = \lambda/kT$, and A and B are the expressions

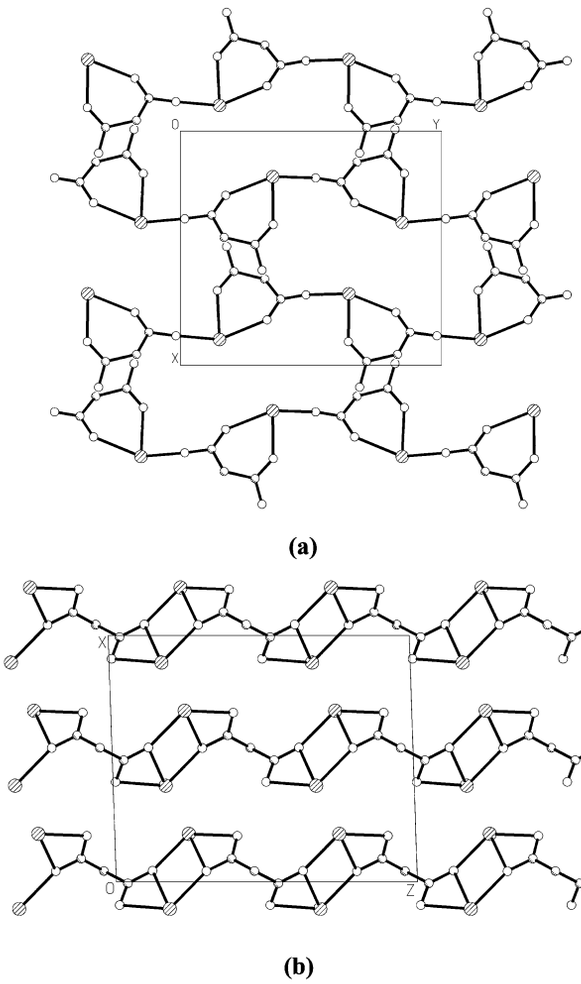

Fig. 5 $[Eu_2(mal)_3(H_2O)_6]$ at 173 K. (a) Projection of the single chains down the *c* axis. Water molecules, malonate ligand L2 and hydrogen atoms have been omitted for clarity. (b) Projection of the double chains down the *b* axis. Water molecules, malonate ligands (L1A and L1B) and hydrogen atoms have been omitted for clarity.

$$A = \left[24 + \frac{(27x-3)}{2e^{-x}} + \frac{(135x-5)}{2e^{-3x}} + (189x-7/2)e^{-6x} + (405x-9/2)e^{-10x} + \frac{(1485x-11)}{2e^{-15x}} + \frac{(2457x-13)}{2e^{-21x}} \right]$$

$$B = [1 + 3e^{-x} + 5e^{-3x} + 7e^{-6x} + 9e^{-10x} + 11e^{-15x} + 13e^{-21x}]$$

The limiting value of χT at high temperatures, $(\chi T)_{HT}$, for $kT \gg \lambda$, can be calculated by means of the following expression for $g_L = 1$ and $g_S = 2$:

$$(\chi T)_{HT} = (N\beta^2/3k)[g_L^2 L(L+1) + g_S^2 S(S+1)]$$

The limit of χT at high temperature is equal to $12N\beta^2/k$, and corresponds to 4.50 $cm^3\ mol^{-1}$ K; although at present this limit has not been reached experimentally. The expected value of χT at low temperatures is zero, since the ground state $^7F_0$ is diamagnetic. Therefore, the value of χT diminishes continuously as the temperature decreases and it approaches the zero value. In practice, the limit of the susceptibility at low temperature is finite and not zero, due to the $\chi(0)$ term which arises through the coupling between the $^7F_0$ and $^7F_1$ states resulting from the second order Zeeman perturbation, whose value depends on λ.

Fig. 7 shows the value of magnetic susceptibility of **1** as a function of temperature. The solid line shows the theoretical behaviour according to eqn. (1) (*vide supra*) computed for λ = 357 cm^{-1}. Although this compound has a dimer structure, in which connections between Eu^{III} ions are formed by μ-oxygens of carboxylate ligands, its magnetic properties have been modelled as if they contained magnetically isolated Eu^{III} ions. The reason for the satisfactory fit obtained presumably relates to the observation that the magnetic interactions in ions of the lanthanide metals (with $4f^n$ valence orbital) are extremely weak. These interactions are pronounced at very low temperatures. In the case of the ion Eu^{III} for $T < 100$ K the only populated state is the ground state which is non-magnetic.

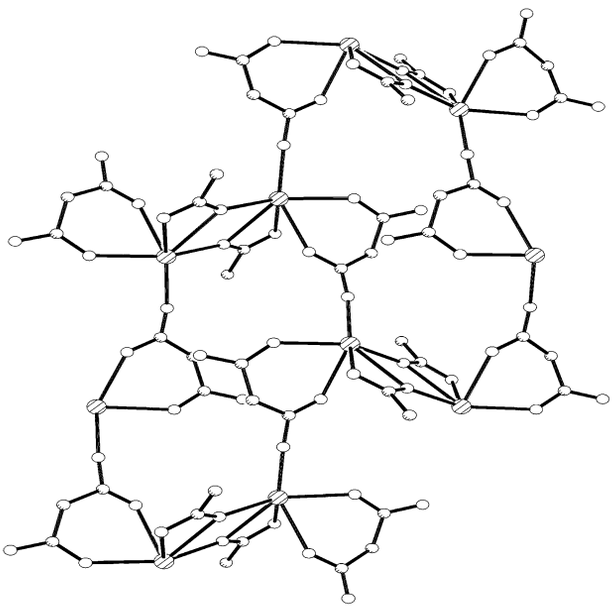

Fig. 6 View of the three-dimensional structure of $[Eu_2(mal)_3(H_2O)_6]$ at 173 K. Water molecules and hydrogen atoms have been omitted for clarity.

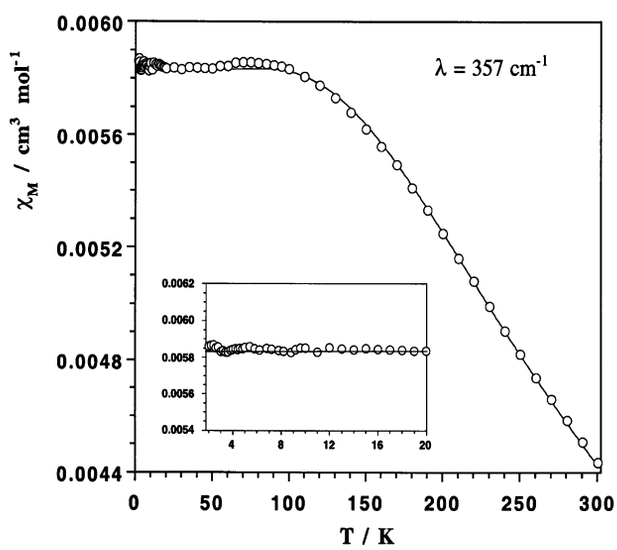

Fig. 7 Thermal dependence of χ_M for $[Eu_2(mal)_3(H_2O)_6]$: (°) experimental data and (—) best-fits through eqn. (1).

Photophysical properties. The Eu^{III} ion has been widely used as a probe to investigate the local structure around rare-earth ions in condensed matter.[12,13] This is due to its relatively simple energy level diagram and the sensitivity of the energy levels and the intensity of its electronic transitions to the local site symmetry and environment at the ions. Moreover, the ground level, $^7F_0$ and the lowest emitting level, $^5D_0$, are non-degenerate, *i.e.*, they are singlets. Thus, the electronic transitions between them are unique and allow one to apply laser-excited site selective spectroscopy to analyse changes from site to site in the energy level diagram, and study lifetime, line width and energy

transfer processes between optical ions and migration of energy between ions in sites close in energy but spectrally different.

In this work, laser-excited site selective spectroscopy has demonstrated that below 236 K the emission bands of the Eu^{III} ions in the crystal are split into two components in a reversible process as a consequence of the presence of two different Eu^{III} sites in the crystal below this temperature.

The emission spectrum of Eu^{III} cations corresponding to transitions $^5D_0 \longrightarrow {}^7F_J$ (J = 0–4) obtained in the complex by exciting at 375 nm at RT is shown in Fig. 8. This spectrum is

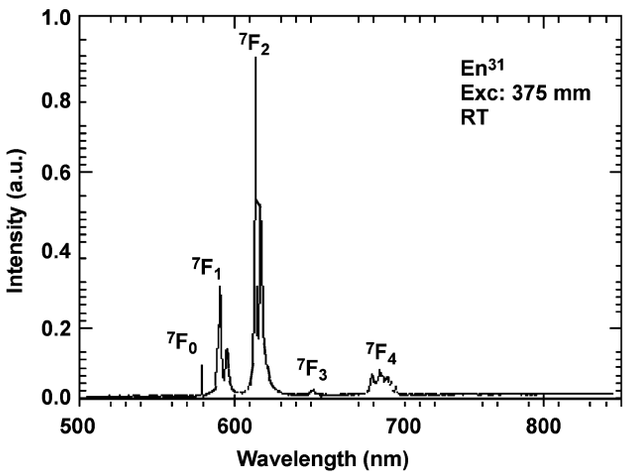

Fig. 8 Emission spectrum of $[Eu_2(mal)_3(H_2O)_6]$ obtained at RT under excitation at 375 nm. All the transitions are from the $5D_0$ level to the indicated levels in the figure.

similar to those obtained for Eu^{III} cations in other crystals.[12,13] The observed emission bands show structure due to the splitting of the ^7F_J levels by the crystal field. Fig. 9 shows the

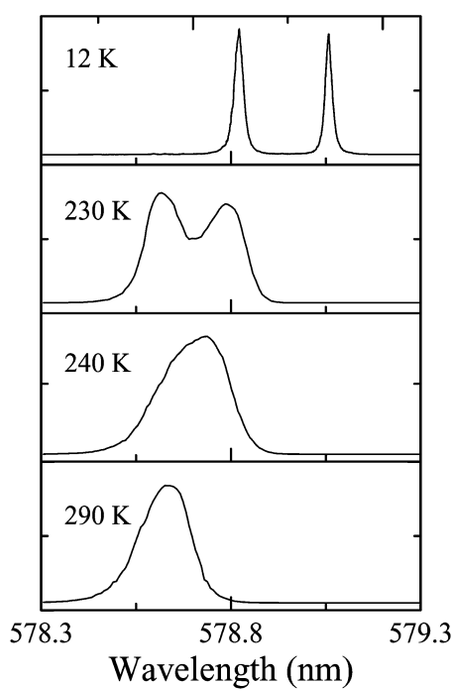

Fig. 9 Excitation spectrum corresponding to the $^7F_0 \longrightarrow {}^5D_0$ transition obtained in the $[Eu_2(mal)_3(H_2O)_6]$ sample at different temperatures.

excitation profile of the $^7F_0 \longrightarrow {}^5D_0$ transition in the range 12–290 K obtained by detecting at 615 nm. At low temperatures (12 K) two peaks are observed. Since the ground and the excited level are both singly degenerate, this result implies the presence of two different crystal-field sites for the Eu^{III} ions at low temperature. When the temperature is increased the width of these peaks increase too, however above 236 K only one peak is observed, indicating the presence of a single crystal-field site for the Eu^{III} cations up to room temperature. The dependence of the peak positions of the $^7F_0 \longrightarrow {}^5D_0$ transition on temperature is shown in Fig. 10.

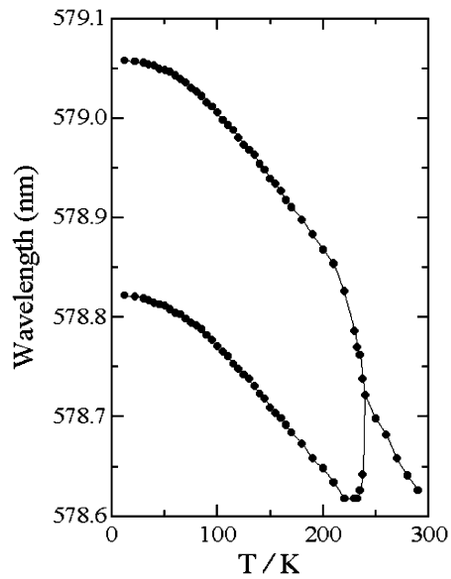

Fig. 10 Dependence of the peak positions of the $^7F_0 \longrightarrow {}^5D_0$ transition on the temperature.

Thermal analyses in the solid phase. The TGA/DSC curves for $[Eu_2(mal)_3(H_2O)_6]$ were measured (Fig. 11a). Decomposition steps were identified using the DTG curve. The TG curve shows a first weight loss in the temperature range from 26 to 228 °C, excluding the possibility of thermal decomposition of the

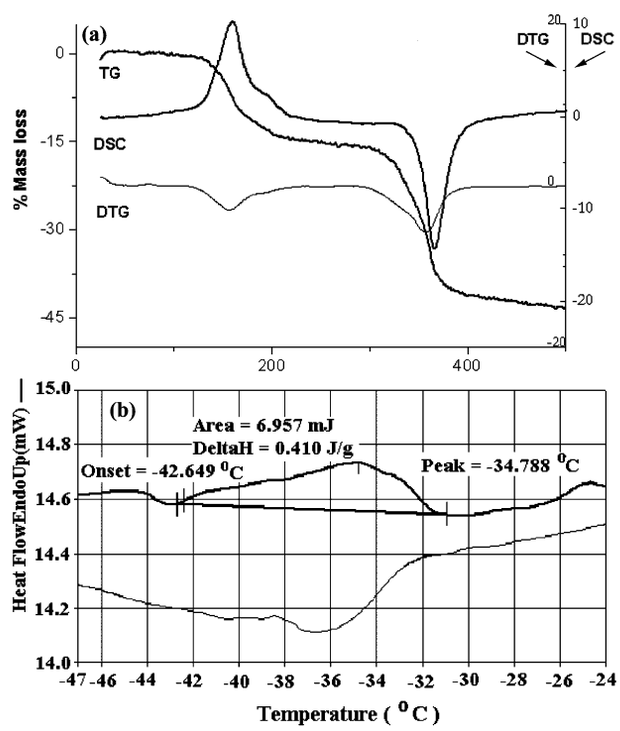

Fig. 11 (a)TG–DSC–DTG curves of $[Eu_2(mal)_3(H_2O)_6]$. All curves have been carried out at 5 °C min^{-1} in a dynamic N_2 atmosphere at 70 cm^3 min^{-1}. TG = % mass loss; DTG = % min^{-1}; DSC = ΔT(μV). (b) DSC curves of $[Eu_2(mal)_3(H_2O)_6]$, increasing and lowering temperatures.

ligand in this temperature range (*vide supra*). A careful look at the TGA–DSC curves shows two endothermic peaks on the DSC curve. One strong, centred at 160 °C, and the other little or a shoulder at 197 °C as a mass loss of 14.97% (TG) {$[T_{peak}]_{DTG}$ = 158 °C} corresponding to the loss of six coordinated water molecules per formula unit (calculated weight loss value 15.04%). The temperatures for weight loss of coordinated water molecules are consistent with other compounds recently reported.[3a,f,5a,9,14,15] After the loss of coordinated water molecules, a strong exothermic peak at 367 °C (DSC) {$[T_{peak}]_{DTG}$ = 357 °C} is observed (Fig. 11a). This peak is due to the start of decarboxylation of the malonic ligand in agreement with other compounds reported involving carboxylate-bridge ligands.[3a,f,5a,9,15] At −42 °C, a phase transition was observed (Fig. 11b).

The absence of thermal hysteresis and the low enthalpy value, may suggest a second order phase transition.

Experimental

Materials

Malonic acid, europium(III) nitrate hexahydrate $Eu(NO_3)_3 \cdot 6H_2O$ and sodium metasilicate nonahydrate $Na_2O_3Si \cdot 9H_2O$ were purchased from commercial sources and used as received. Elemental analysis (C, H) were performed with an EA 1108 CHNS-0 automatic analyser.

Physical techniques

Variable-temperature (1.9–290 K) magnetic susceptibility measurements were carried out on polycrystalline samples with a Quantum Design SQUID magnetometer operating at 100 (T < 50 K) and 1000 G (over all the temperature range). The susceptibility data were corrected for the diamagnetism of the constituent atoms. Broad band emission spectra were obtained by exciting the samples with light from a 250 W incandescent lamp passed through a 0.25 m monochromator. Fluorescence was detected through a 0.25 m double monochromator with a photomultiplier. For laser-excited site selective spectra a tunable dye laser operating with Rhodamine 6G (spectral line width 0.15 cm^{-1} and pulse width 5 ns), pumped by a Q-switched 532 nm frequency-doubled Nd–YAG laser, was used. For low temperature measurements, a continuous flow helium cryostat was used in the range 12 to 290 K. Thermal studies were carried out with a Netzsch STA 409 EP simultaneous thermal analyser. A 5.5 mg pure sample was subjected to dynamic TG and DSC scans at a heating rate of 5 °C min^{-1} in a nitrogen atmosphere (70 cm^3 min^{-1}), in the range from ambient to 400 °C. The TG curves were analysed as percentage mass loss as a function of temperature. The number of descomposition steps was identified using the derivative thermogravimetric curve (DTG). The DSC curves were analysed as differential scanning calorimetric [ΔT(μV)]. Differential scanning calorimetry (DSC) at low temperatures was performed on Perkin-Elmer Pyris 1 equipment, from 25 to −175 °C, with a 10 °C min^{-1} flow rate, and helium as purge gas. Such measurements were carried out both during the warming and the cooling process.

Synthesis of $[Eu_2(mal)_3(H_2O)_6]$

The formation of this europium malonate is accomplished by the reaction between malonic acid and europium nitrate in sodium metasilicate gels. The silica gels were prepared by hydrolysis and polycondensation of sodium metasilicate nonahydrate in water solution under acidic conditions.[16] Preparation primarily involved mixing of appropriate amounts of $Na_2SiO_3 \cdot 9H_2O$, 1 M, and 2 M malonic acid, to adjust the pH value of the mixed solutions to about 4.5. The mixture was run into test tubes, covered, and allowed to set for 24 hours at room temperature. A solution of europium nitrate hexahydrate (0.5 M), was added on top of the gel dropwise, so that the surface of the gel would not break, and the tubes were stored at 30 °C. Three weeks later, colourless crystals appeared suitable for X-ray analysis. They were removed from the gel, washed and dried at room temperature. (Found: C, 15.14; H, 2.47. Calc. for $C_9H_{18}Eu_2O_{18}$: C, 15.05; H, 2.53%).

The compound $[Eu_2(mal)_3(H_2O)_5] \cdot 3H_2O$[6] was precipitated from a solution containing europium(III) chloride, malonic acid and sodium hydroxide. This method of synthesis produces a species that is more hydrated than the one described in this work. Here the formation of the hexahydrate europium malonate $[Eu_2(mal)_3(H_2O)_6]$ is accomplished by reaction between malonic acid and europium nitrate in sodium metasilicate.

Table 2 Crystal data and structure refinement for $[Eu_2(mal)_3(H_2O)_6]$

	293 K	173 K
Empirical formula	$C_9H_{18}O_{18}Eu_2$	$C_9H_{18}O_{18}Eu_2$
Formula weight	718.15	718.15
Crystal system	Monoclinic	Monoclinic
Space group	*I*2/*a*	*Ia*
a/Å	11.094(6)	11.0504(12)
b/Å	12.246(4)	12.2959(16)
c/Å	13.581(6)	13.4671(3)
β/°	93.00(3)	91.915(16)
V/Å^3	1842.5(14)	1828.82(5)
Z	4	4
μ/mm^{-1}	6.838	6.890
R(int)	0.0168	0.0219
No. of reflections/observed	1625/1624	2940/2741
*R*1 [$I > 2\sigma(I)$]	0.0332	0.0190
*wR*2 [$I > 2\sigma(I)$]	0.0942	0.0411

Crystallographic data collection at 293 K

A crystal of dimensions 0.4 × 0.55 × 0.20 mm was used for data collection on an Enraf-Nonius MACH-3 four-circle diffractometer. Orientation matrix and lattice parameters were obtained by least-squares refinement of the diffraction data of 25 reflections within the range 6 < θ < 18°.[17,18] Data were collected at 293(2) K using graphite-monochromated Mo-Kα radiation (λ = 0.71073 Å) and the ω-scan technique. A summary of the crystallographic data and structure refinement is given in Table 2. Examination of three standard reflections, monitored every two hours, showed no sign of crystal deterioration. The index ranges of data collection were $0 \le h \le 23$, $0 \le k \le 17$, $-15 \le l \le 12$. Of the 2661 measured independent reflections in the θ range 3.00–29.97°, 2650 have $I \ge 2\sigma(I)$. All the measured independent reflections were used in the analysis. Intensity data were corrected for Lorentz-polarization and absorption.[19] The maximum and minimum effective transmission factors were 2.065 and 0.585, respectively.

Crystallographic data collection at 173 K

A single crystal of dimensions 0.4 × 0.2 × 0.2 mm was then mounted on a glass fibre using inert vacuum grease and transferred to the cold gas stream of the diffractometer. The space group was determined by careful comparison between structure refinements in the centrosymmetric space group *I*2/*a* and the non-centrosymmetric space groups *I*a and *I*2. Intensity statistics do not clearly distinguish between centrosymmetric and non-centrosymmetric options here ($\langle|E^2 - 1|\rangle$ = 0.886). Similarly, *h*0*l* reflection intensities do not unambiguously determine the space group. Thus *h*0*l* ($h = 2n + 1$) reflections are generally very weak ($\langle I\rangle$ = 0.9 where $\langle I\rangle$ for all reflections = 122.1). Therefore it seems likely that the space group is *Ia* (or *I*2/*a*) rather than *I*2. Table 3 shows the results of the comparison of refinement in all three space groups, which indicate that the structure is best described in *Ia* with inversion twinning. This is consistent with

Table 3 A comparison between refinements in centrosymmetric and non-centrosymmetric space groups for $[Eu_2(mal)_3(H_2O)_6]$ at 173 K

	*I*2/*a*	*Ia*	*I*2
*R*1	0.0309	0.0190	0.0330
*wR*2	0.0675	0.0411	0.0876
GOOF	1.453	0.964	1.020
Weighting (a,b)[a]	0.1381, 7.9210	0.0138, 0.0	0.0416, 55.1296
Fourier peaks	0.83,0.80 (−1.03)	1.12, 0.80 (−0.98)	1.49, 0.99 (−0.80)
Extinction coefficient	0.00212(13)	0.00172(5)	0.00174(13)
Non-positive definite atoms	None	None	21
Isotropic constraints/restraints	O1W′ fully isotropic	None	None
Geometry restraints	All H_2O hydrogens	None	None
Disorder/comments on refinement	O1W: 2 sites of occupancy 0.76(9) and 0.24(9)	None	O105 disordered, hydrogens not located or refined
R(int)	0.0247	0.0219	0.0235
Flack parameter	N/A	0.48(3)	0.45(6)
No. of reflections collected	4749	4749	4749
No. of unique reflections	1611	2940	2431
No. of least squares parameters	156	300	252
No. of correlation matrix elements > 0.75	1	>24	24

[a] $w = 1/[\sigma^2(F_o^2) + (aP)^2 + bP]$; $P = [2F_c^2 + \max(F_o^2,0)]/3$.

the spectroscopic data given elsewhere in this paper. Details of the structure determinations are listed in Table 2.

Structure determination

The structures were solved by direct methods and refined with full-matrix least-squares technique on F^2 using the SHELXS-97[20] and SHELXL-97[21] programs. All non-hydrogen atoms were refined anisotropically. At 293 K the hydrogen atoms of malonate ligand were set in calculated positions and isotropically refined; the hydrogen atoms of water molecules were not found. At 173 K all hydrogen atoms were located in the electron density difference map, and isotropically refined. The final full-matrix least-squares refinement was performed minimising the function $\Sigma\omega(|F_o|^2 - |F|^2)$ with $\omega = 1/[\sigma^2(F_o)^2 + mP^2 + nP]$ and $P = (F_o^2 + 2F_c^2)/3$ with $m = 0.0383$ (293 K) and 0.0317 (173 K) and $n = 27.2802$ (293 K) and 0.000 (173 K). The values of the discrepancy indices $R1$ (R_{w2}) for all data were 0.0318 (0.0858) at 293 K and 0.0214 (0.0452) at 173 K, whereas those listed in Table 3 correspond to the data with $I > 2\sigma(I)$. The final Fourier-difference map showed maximum and minimum height peaks of 1.399 and −1.312 e Å^{-3} at 293 K and 1.12 and −0.98 e Å^{-3} at 173 K. The values of number of reflections/number of variable parameters are 133 at 293 K and 336 at 173 K, and those of the goodness-of-fit are 1.239 at 293 K and 0.725 at 173 K. The final geometrical calculations and the graphical manipulations were carried out with PARST95[22] and PLATON[23] programs, respectively.

CCDC reference numbers 181893 and 181894.

See http://www.rsc.org/suppdata/dt/b2/b202649j/ for crystallographic data in CIF or other electronic format.

Conclusions

Our studies on the coordinating ability of the malonate dianion show that its great versatility as a ligand allow the construction of extended networks with different topologies which are dependent on the coordination geometry of the metal ion and on the end-cap ligand previously bound to it, as shown in Scheme 1. Study of the new three-dimensional compound of formula $[Eu_2(mal)_3(H_2O)_6]$ reported herein allowed us to establish the conclusions listed below:

(1) This compound crystallizes in the monoclinic system and exhibits a phase transition as a function of temperature. At both 293 and 173 K, nine oxygen atoms form a distorted monocapped square antiprism which surrounds the Eu^{3+} ions and the crystal structures are stabilised through extensive hydrogen bonding involving carboxylate and water molecules.

(2) Analysis of the magnetic behaviour of this compound as a function of temperature reveals the lack of significant magnetic interactions between the spins of the Eu(III) cations through the bridging carboxylate-oxygens.

(3) Laser-excited site selective spectroscopy has demonstrated that below 236 K the emission bands of the Eu^{III} ions in the crystal are split into two components in a reversible process as a consequence of the presence of two different Eu^{III} sites in the crystal below this temperature.

(4) The absence of thermal hysteresis and the low enthalpy value, may suggest a second order phase transition.

Acknowledgements

Support from Gobierno Autónomo de Canarias (project PI2000/135), the University of Bristol, and the Spanish Ministery of Science and Technology (project BQU2001-3794) is gratefully acknowledged.

References

1 G. R. Desiraju (ed.), *The Crystal as a Supramolecular Entity*, Wiley, New York, 1995.
2 R. Robson, B. F. Abrahams, S. R. Batten, R. W. Gable, B. F. Hoskins and J. Liu, *Supramolecular Architecture*, ACS, Washington, DC, 1992.
3 (*a*) M. Hernández-Molina, P. A. Lorenzo-Luis, T. López, C. Ruiz-Pérez, F. Lloret and M. Julve, *CrystEngComm*, 2000, **31**, 1; and references therein; (*b*) C. Ruiz-Pérez, J. Sanchiz, M. Hernández-Molina, F. Lloret and M. Julve, *Inorg. Chem.*, 2000, **39**, 1363; (*c*) C. Ruiz-Pérez, M. Hernández-Molina, P. A. Lorenzo-Luis, F. Lloret, J. Cano and M. Julve, *Inorg. Chem.*, 2000, **39**, 3845; (*d*) C. Ruiz-Pérez, J. Sanchiz, M. Hernández-Molina, F. Lloret and M. Julve, *Inorg. Chim. Acta*, 2000, **298**, 202; (*e*) C. Ruiz-Pérez, M. Hernández-Molina, J. Sanchiz, T. López, F. Lloret and M. Julve, *Inorg. Chim. Acta*, 2000, **298**, 245; (*f*) M. Hernández-Molina, P. A. Lorenzo-Luis, C. Ruiz-Pérez, F. Lloret and M. Julve, *Inorg. Chim. Acta*, 2001, **313**, 87; (*g*) Y. Rodríguez-Martín, C. Ruiz-Pérez, J. Sanchiz, F. Lloret and M. Julve, *Inorg. Chim. Acta*, 2001, **318**, 159; (*h*) J. Sanchiz, Y. Rodríguez-Martín, A. Mederos, C. Ruiz-Pérez, F. Lloret and M. Julve, *New J. Chem.*, 2002, **26**, DOI: 10.1039/b201849g; (*i*) Y. Rodríguez-Martín, M. Hernández-Molina, F. S. Delgado, J. Pásan, C. Ruiz-Pérez, J. Sanchiz, F. Lloret and M. Julve, *CrystEngComm*, 2002, **4**(73), 440; (*j*) A. Cabeza, M. A. G. Aranda and S. Bruque, *J. Mater. Chem.*, 1999, **9**, 571.
4 Z. M. Wang, L. J. van de Burgt and G. R. Choppin, *Inorg. Chim. Acta*, 2000, **310**, 248.
5 (*a*) M. Insausti, R. Cortés, M. I. Arriortua, T. Rojo and E. H. Bocanegra, *Solid State Ionics*, 1993, **63–65**, 351; (*b*) J. García-Jaca, J. I. R. Larramendi, M. Insausti, M. I. Arriortua and T. Rojo, *J. Mater. Chem.*, 1995, **5**, 1995; (*c*) I. G. Muro, F. A. Mautner,

M. Insausti, L. Lezama, M. I. Arriortua and T. Rojo, *Inorg. Chem.*, 1998, **37**, 3243; (*d*) I. G. de Muro, M. Insausti, L. Lezama, J. L. Pizarro, M. I. Arriortua and T. Rojo, *Eur. J. Inorg. Chem.*, 1999, 935.
6 E. Hansson, *Acta Chem. Scand.*, 1973, **27**, 2827.
7 (*a*) E. Hansson, *Acta Chem. Scand.*, 1973, **27**, 2441; (*b*) E. Hansson, *Acta Chem. Scand.*, 1973, **27**, 2841.
8 X. Wein Mei, W. Qiguang, Y. Lan and Y. Rudong, *Polyhedron*, 1992, **11**, 2051.
9 F. Marrot and J. C. Trombe, *Polyhedron*, 1994, **13(12)**, 1931.
10 B. Benmerad, A. Guehria-Laïdoudi, G. Bernadinelli and F. Balegroune, *Acta Crystallogr., Sect. C*, 2000, **56**, 321.
11 (*a*) O. Kahn, *Molecular Magnetism*, VCH, Weinheim, 1993, pp. 48 and 49; (*b*) J. H. Van Bleck and A. Frank, *Phys. Rev.*, 1929, **34**, 1494; (*c*) J. H. Van Bleck and A. Frank, *Phys. Rev.*, 1929, **34**, 1625.
12 M. Buijis, G. Blasse and L. H. Brixner, *Phys. Rev. B*, 1986, **34**, 8815.
13 J. E. Muñoz Santiuste, N. Macalik and J. García Solé, *Phys. Rev. B*, 1993, **47**, 88.
14 (*a*) F. Cecconi, C. A. Ghilardi, P. Gili, S. Midollini, P. A. Lorenzo Luis, A. D. Lozano-Gorrín and A. Orlandini, *Inorg. Chim. Acta*, 2001, **319**, 67; (*b*) Y. B. Dong, M. D. Smith, R. C. Layland and H. C. Loye, *J. Chem. Soc., Dalton Trans.*, 2000, 775; J. G. Kang, S. K. Yoon, Y. Sohn, J. G. Kim, Y. D. Kim and II. H. Suh, *J. Chem. Soc., Dalton Trans.*, 1999, 1467; (*c*) B. L. Chen, K. F. Mok, S. C. Ng and M. G. B. Drew, *New. J. Chem.*, 1999, **23**, 877; (*d*) G. B. Hix, S. J. Kitchin and K. D. M. Harris, *J. Chem. Soc., Dalton Trans.*, 1998, 2315.
15 (*a*) Y. Rodríguez-Martín, P. Lorenzo-Luis and C. Ruiz-Pérez, *Inorg. Chim. Acta*, 2002, **328**, 169; (*b*) J. Novosad, A. C. Messimeri, C. D. Papadimitriou, P. G. Veltsistas and J. D. Woollins, *Transition Met. Chem.*, 2000, **25**, 664.
16 H. K. Henisch, *Crystal Growth in Gels*, The Pennsylvania State University Press, Pittsburgh, 1970.
17 Enraf-Nonius, CAD-4 EXPRESS, Version 5.1/5.2, Enraf-Nonius, Delft, The Netherlands, 1994.
18 A. L. Spek, HELENA: Program for Data Reduction, Utrecht University, The Netherlands, 1997.
19 J. González-Platas, and C. Ruiz-Pérez, NEWCORR: Program for Empirical Correction, University of La Laguna, La Laguna, Spain, 1997.
20 G. M. Sheldrick, SHELXS-97, University of Göttingen, Germany. 1997.
21 G. M. Sheldrick, SHELXL-97, Program for the Refinement of Crystal Structure, University of Göttingen, Germany. 1997.
22 PARST95 (An update to PARST) a system of Fortran routines for calculating molecular structure parameters from the results of crystal structure analyses. M. Nardelli, *J. Appl. Crystallogr.*, 1995, **28**, 659.
23 A. L. Spek, *Acta Crystallogr., Sect. A*, 1990, **46**, C-34.